Magnetic Resonance in Medicine 62:975–983 (2009)

Assessment of Myocardial Blood Flow (MBF) in Humans Using Arterial Spin Labeling (ASL): Feasibility and Noise Analysis

Zungho Zun,[1*] Eric C. Wong,[2,3] and Krishna S. Nayak[1]

Arterial spin labeling (ASL) is a powerful tool for the quantitative measurement of tissue blood flow, and has been extensively applied to the brain, lungs, and kidneys. ASL has been recently applied to myocardial blood flow (MBF) measurement in small animals; however, its use in humans is limited by inadequate signal-to-noise ratio (SNR) efficiency and timing restrictions related to cardiac motion. We present preliminary results demonstrating MBF measurement in humans, using cardiac-gated flow-sensitive alternating inversion recovery (FAIR) tagging and balanced steady-state free precession (SSFP) imaging at 3T, and present an analysis of thermal and physiological noise and their impact on MBF measurement error. Measured MBF values in healthy volunteers were 1.36 ± 0.40 ml/ml/min at rest, matching the published literature based on quantitative ^{13}N-ammonia positron emission tomography (PET), and increased by 30% and 29% with passive leg elevation and isometric handgrip stress, respectively. With thermal noise alone, MBF can be quantified to within ± 0.1 ml/ml/min with 85.5% confidence, for 3.09 cm^3 regions averaged over 6 breath-holds. This study demonstrates the feasibility of quantitative assessment of myocardial blood flow in humans using ASL, and identifies SNR improvement and the reduction of physiological noise as key areas for future development. Magn Reson Med 62: 975–983, 2009. © 2009 Wiley-Liss, Inc.

Key words: myocardial perfusion imaging; myocardial blood flow; arterial spin labeling; FAIR; SSFP

Myocardial perfusion imaging (MPI) plays an essential role in the diagnosis and risk assessment of patients with coronary artery disease (CAD). While coronary angiography provides an assessment of the coronary artery lumen, MPI provides a direct assessment of the physiological significance of the disease that may lead to clinical symptoms, electrocardiogram (ECG) changes, and eventually ischemic events and outcomes. Its importance is underscored by the fact that roughly 10 million single-photon emission computed tomography (SPECT) MPI scans are performed each year in the United States alone. MRI-based first-pass methods are widely used (1–4) and provide a means to qualitatively assess myocardial perfusion with higher spatial resolution than SPECT. These methods, while promising, have key limitations that include unresolved artifacts (e.g., dark rim) (5), difficulties with inter-observer variability (6) and absolute quantification of MBF, and the toxic syndrome known as nephrogenic fibrosing dermopathy in patients with end-stage renal disease (7).

Over the past several years, arterial spin labeling (ASL) has developed into a powerful tool for the quantitative measurement of tissue blood flow using MRI, and has been primarily applied to the brain. In this approach, radiofrequency pulses are used to modify the longitudinal magnetization of arterial blood, generating an endogenous tag that decays away with a time constant given by the T_1 relaxation rate (≈1.5 s for blood at 3T (8)). Images of the target tissue are obtained both with and without the preparation, and tissue blood flow and other parameters can be extracted from signal differences. ASL has two key advantages compared to other perfusion imaging techniques, including MRI-based first-pass methods. First, the ASL signal is inherently and quantitatively related to tissue blood flow. Because the decay of the tag is rapid, images must be acquired within a few seconds of the application of the tag, and there is insufficient time for the tag to leave the target tissue by venous outflow. Fast exchange of tagged blood water with tissue water further decreases the likelihood of washout. This results in a tracer technique in which the tag is effectively trapped in the target tissue, similar to the classic microsphere-based blood flow measurement. Second, ASL MRI is completely noninvasive, and does not require intravenous infusion of paramagnetic contrast agents or exposure to ionizing radiation. It therefore poses no risk to the patient (above that of a conventional MRI scan) and can be repeated indefinitely, opening new opportunities for repeated or even continuous monitoring of patients as they undergo treatment.

Compared to brain ASL, myocardial ASL faces several unique challenges. Cardiac motion requires the gating of tagging and imaging to appropriate portions of the cardiac cycle, rapid imaging during the stable cardiac phases (mid-diastole or end-systole), and limits the tag delay to an integer number of R-R intervals for most ASL tagging schemes. Respiratory motion requires the acquisition of tagged and control image pairs during the same breath-hold, during synchronized breathing, and/or with careful image registration. The cardiac geometry complicates the location and timing of tagging, and leads to a high apparent ASL signal in the left ventricular (LV) blood pool with conventional tagging schemes (e.g., pulsed slab, continuous). Finally, the intrinsic myocardial signal-to-noise ratio (SNR) achieved with modern cardiac phased-array coils is roughly three times lower than the intrinsic gray matter

[1]Ming Hsieh Department of Electrical Engineering, Viterbi School of Engineering, University of Southern California, Los Angeles, California, USA.

[2]Department of Radiology, University of California, San Diego, San Diego, California, USA.

[3]Department of Psychiatry, University of California, San Diego, San Diego, California, USA.

*Correspondence to: Zungho Zun, Research Assistant, 3740 McClintock Ave, EEB 412, University of Southern California, Los Angeles, CA 90089-2564. E-mail: zun@usc.edu

Received 10 October 2008; revised 16 April 2009; accepted 21 April 2009.

DOI 10.1002/mrm.22088

Published online 11 August 2009 in Wiley InterScience (www.interscience.wiley.com).

SNR achieved with modern head coils, leading to a significant increase in the number of averages required for reliable tissue blood flow quantification.

Previous attempts at myocardial ASL have been successful in small animals (9,10) where SNR is high due to local radio frequency (RF) coils, and heart rates are high, enabling apparent T_1 mapping (11) to be performed (i.e., the T_1 recovery curve can be sampled at many time points, each during a stable cardiac phase). In contrast, the development of human myocardial ASL is still at an early stage (12–16). Preliminary studies have been mostly based on flow-sensitive alternating inversion recovery (FAIR) (17,18), and differ in the models used for quantification and the methods used for breathing control and image acquisition. Wacker et al. (12) utilized apparent T_1 measurement after a saturation pulse (instead of an inversion pulse), which avoids the need for full relaxation between measurements, leading to reduced scan time and improved performance in the presence of irregular heart rates. Zhang et al. (13,14) acquired sets of images following a single inversion pulse for apparent T_1 measurement, accounting for magnetization saturation effects due to imaging excitation, and demonstrated this approach in dogs (13) and humans (14). Poncelet et al. (15) utilized a quantification model derived from the Bloch equation, along with synchronized breathing, double-gating, and echo-planar imaging (EPI) image acquisition. A data fitting procedure was used to extrapolate the ASL signal from data acquired with different inversion times (caused by variations in heart rate). An et al. (16) employed a similar quantification model using FAIR tagging and balanced steady-state free precession (SSFP) image acquisition, and performed image acquisition in a pseudosteady state, assuming constant heart rate. Despite these attempts, no robust ASL methods for the measurement of MBF in humans have been described, and we focus here on an analysis of the signal stability required for such measurements.

We demonstrate the feasibility of MBF measurement in humans, using breathheld cardiac-gated FAIR tagging and SSFP imaging at 3T, and present an analysis of thermal and physiological noise and their impact on MBF measurement error. Resting MBF measurements in 10 healthy volunteers match ranges established using quantitative ^{13}N-ammonia positron emission tomography (PET). The myocardial ASL signal was found to be inflow-dependent, and was found to increase with passive leg elevation and isometric handgrip stress. We also determine that myocardial ASL is critically limited by SNR and physiological noise, which are important challenges for further investigation.

MATERIALS AND METHODS

Pulse Sequence

Myocardial ASL was performed using a cardiac-gated FAIR-SSFP (16,19) pulse sequence illustrated in Fig. 1. FAIR tagging utilizes slab-selective and nonselective inversion pulses applied alternately to generate control images (without inversion of out-of-slice blood) and tagged images (with inversion of out-of-slice blood), respectively. Inversion and imaging are both centered at the same cardiac phase (mid-diastole, as determined by cinema/video [CINE] scout scan) in successive R-R intervals such that the inversion slab contains the imaging slice, and the estimated MBF provides the average perfusion rate of pulsatile blood flow over one R-R interval. One pair of control and tagged images was acquired during a single breathhold to minimize spatial misregistration during subtraction. There was a 6-s time delay between the two image acquisitions, to allow for near-complete recovery of longitudinal magnetization. Six breathholds (~10–12 s each) were performed to enable signal averaging of the tagged and control images. One short breathhold (<3 s) was performed to acquire a baseline image (i.e., with no preparation) for quantification. The time delay between breathholds was kept ≥15 s to ensure complete recovery of longitudinal magnetization. The subject's heart rate was monitored, and pulse timings were adjusted in real-time to follow the appropriate cardiac phase. To achieve complete cancellation of static tissue signal during subtraction, the inversion delay was kept identical for each image pair obtained in the same breathhold. If there was a change in heart rate during the breathhold, the timing of the inversion pulse prior to the second image acquisition was shifted slightly, and for all practical purposes, still occurred during diastasis. The order of control and tagged image acquisition was alternated in each breathhold and an even number of repetitions was used, in order to eliminate any bias due to incomplete recovery.

Image acquisition was performed using a snapshot two-dimensional Fourier transform (2DFT) balanced SSFP sequence with TR = 3.2 ms (total duration = 313 ms), 50° prescribed flip angle, and linear view ordering with full *k*-space acquisition. A five-tip linear ramp was used to reduce signal oscillations during the transient SSFP acquisition (20,21). In each study, a single mid-short-axis slice was imaged using a 96 × 96 matrix over a 20-cm–24-cm isotropic field of view (FOV), with slice thickness = 10 mm. Acquisitions were prospectively gated using ECG or photoplethysmograph signals. Inversions were achieved using adiabatic (hyperbolic secant) pulses because of their insensitivity to B_0 and B_1 variation. For slab-selective inversion, a thickness of 30 mm was used to trade off tolerance to slice profile imperfections and reduction of transit delay.

Reconstruction

Images were reconstructed using sensitivity encoding (SENSE) (22) with the reduction factor, R = 1, also known as optimal B_1 reconstruction (OBR) (23,24). Thus, SENSE reconstruction was used not for acceleration but to optimally combine signal from all coils and produce real-valued images that retain Gaussian image statistics even when the signal amplitude is close to zero. Note that in low SNR cases, sum-of-squares reconstruction results in an image signal that follows a noncentral chi distribution. Coil sensitivity maps and the channel noise covariance matrix were obtained in a standard way (22) prior to ASL imaging.

Quantification

Regions of septal myocardium were manually segmented for each breathhold, based on the difference signal (control

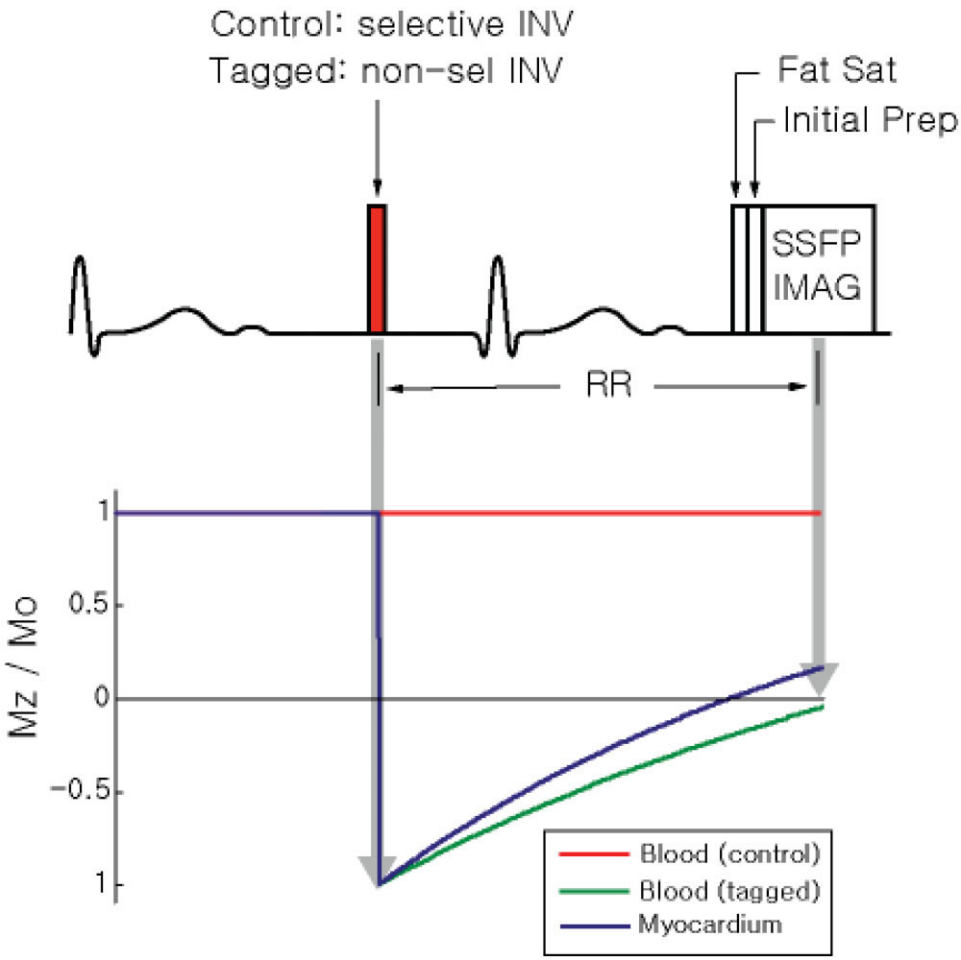

FIG. 1. Myocardial ASL pulse sequence. Tagging and imaging are both centered at mid-diastole. Using flow-induced alternating inversion recovery (FAIR), preparatory inversion pulses are either slab-selective or nonselective to generate control or tagged images, respectively. Imaging is performed using a snapshot balanced steady-state free precession (SSFP) sequence that is preceded by fat saturation, to reduce signal from epicardial fat, and a five-tip linear ramp preparation, to minimize transient signal oscillations. During each breathhold, one control image and one tagged image are acquired with a 6-s pause between.

– tagged). Regional MBF was estimated using the following equation:

$$MBF = \frac{C - T}{2B \cdot RR \cdot e^{-RR/T_1}}, \quad [1]$$

derived from Buxton's general kinetic model (25), where C, T, and B refer to the mean myocardial signal on the region of interest (ROI) in the control, tagged, and baseline images, RR represents the interval between two consecutive R waves, and T_1 corresponds to the T_1 of blood. Signal averaging was performed over voxels within an ROI as well as over multiple breathholds to increase SNR.

Thermal Noise Analysis

Tagged and control images will each be corrupted by thermal noise, which will propagate to the MBF measurement. For Cartesian acquisitions, thermal noise is independent and identically distributed (i.i.d.) additive white Gaussian in the image domain. Consider σ_N to be the noise standard deviation (SD) for each voxel in each source image (tagged and control). $C - T$ in Eq. [1] can be considered a random variable with a standard deviation $\sqrt{2} \cdot \sigma_N$ for each voxel. When signals are averaged over N_{avg} voxels (e.g., over a spatial region and/or multiple breathholds), the SD of $C - T$ becomes $\sqrt{2/N_{avg}} \cdot \sigma_N$. Therefore, the measured MBF error (ΔMBF) is expected to follow a Gaussian distribution, with zero mean and SD:

$$\sigma_{MBF,T} = \frac{\sqrt{2/N_{avg}} \cdot \sigma_N}{2B \cdot RR \cdot e^{-RR/T_1}}, \quad [2]$$

where variations in B can be neglected because of the high SNR of baseline images (>40 in our studies). For a given SNR, RR interval, and T_1 of blood, Eq. [2] relates the number of averages, N_{avg} to the distribution of measured MBF error. We calculated the minimum number of voxels to be averaged such that the measured MBF error is <0.1 ml/ml/min with >90% confidence. With SNR = 70, heart rate = 60 bpm, and T_1 of blood = 1660 ms, this minimum number is about 300. In order to achieve close to this number of voxels over a septal ROI, we acquired six tagged and control image pairs during six breathholds, with about 50 voxels in the prescribed ROI for each breathhold for all scans. MBF measurement confidences were reexamined after the scan using the actual ROI sizes and the measured SNR for each subject.

Physiological Noise Analysis

One of the critical sources of errors in myocardial ASL is the physiological noise caused by metabolic fluctuation,

respiratory and cardiac motion, and other unknown variations over time. The variance of MBF measurements from each of the six breathholds was calculated to estimate the temporal variation of the measurements. For the offset caused by alternating control/tagged imaging order to be excluded from the variance estimation, the variance of six measurements, σ_S^2 was calculated as follows.

$$\sigma_S^2 = \frac{\sigma_{odd}^2 + \sigma_{even}^2}{2}, \quad [3]$$

where σ_{odd}^2 is a variance of average MBF from the first, third, and fifth breathholds (tagged image acquired before control image), and σ_{even}^2 is a variance of average MBF from the second, fourth, and sixth breathholds (control image acquired before tagged image). Based on the Gaussian model of physiological noise, the measured MBF error averaged from six breathholds follows a Gaussian distribution with zero mean and SD:

$$\sigma_{MBF,P} = \frac{\sigma_S}{\sqrt{N_{BH}}}, \quad [4]$$

where N_{BH} is the number of breathholds, which was six for all scans. The probability of measured MBF error being <0.1 ml/ml/min was recalculated using this distribution.

Experimental Methods

Experiments were performed on two 3T whole-body short-bore scanners (Signa Excite HD; GE Healthcare, Waukesha, WI, USA) with gradients supporting 40 mT/m amplitude and 150 mT/m/ms slew rate. The body coil and an eight-channel cardiac array coil were used for RF transmission and signal reception, respectively. Each subject was screened and provided informed consent in accordance with institutional policy.

Resting MBF

Resting MBF measurements were performed in 10 healthy volunteers (8 males/2 females, ages 28–35 years, heart rate = 50–76 bpm). Five of the subjects were imaged twice on separate days, resulting in 15 total scan sessions. No restriction was placed on exercise or caffeine/food intake prior to imaging.

Dependence on Inflow

In five healthy subjects, myocardial ASL scans were performed with three different tagging regions. In these three scans, the thickness of the selective inversion used for the control image was modified to include either: Case 1) only the imaging slice (3 cm thick); Case 2) the entire LV myocardium up to the aortic valve plane (12 cm thick); or Case 3) everything (nonselective). Increasing the thickness of the slab-selective inversion reduces the tagged blood volume, and is expected to reduce the measured MBF. Case 2 excludes blood already in the coronary vasculature. Case 3 excludes all blood, leading to an expected MBF measurement of zero.

Modulation with Mild Stress

In seven healthy subjects, myocardial ASL scans were performed at rest, and with two forms of mild stress: leg elevation and handgrip. For leg elevation, both of the subjects' legs were passively elevated by 30–40 degrees to increase venous return. Leg elevation started 5 min before scanning and was maintained throughout the ASL scan. For handgrip stress, the subjects were asked to maintain isometric handgrip at 40% of maximum voluntary contraction (MVC) (26,27). Handgrip was initiated 1–2 min before each ASL scan, was maintained throughout the ASL scan, and was monitored by a handgrip dynamometer. MBF during handgrip is expected to be roughly 35% higher than at rest (28). Aortic blood flow (ABF) during leg elevation is expected to be roughly 16% higher than at rest, which likely also results in increased MBF (29). For this study only, subjects were asked to refrain from caffeine or food intake for 4 h prior to the scan, because they can increase resting MBF, and reduce the amount of MBF modulation caused by these stressors.

RESULTS

Resting MBF

The measured resting MBF, SD of MBF error, and confidences for MBF error <0.1 ml/ml/min based on thermal noise only and physiological noise are summarized in Table 1. The measured MBF range was 0.74–2.25 ml/ml/min, which is consistent with the quantitative ^{13}N-ammonia PET literature that has reported 0.73–2.43 ml/g/min as a range for asymptomatic human subjects (30). The confidence based on thermal noise only was in a range of 70.0–98.5%. This variation can be largely explained by the variation in intrinsic SNR and the variation in septal ROI size across subjects. The septal ROI size ranged from 1.35 to 6.53 cm^3, where smaller septal ROIs were used in subjects with thinner myocardium. The confidence based on physiological noise was 18.2–94.0%, showing a substantially wider range compared to that of thermal noise. The SD of MBF error due to thermal noise only and physiological noise were 0.0682 ± 0.0186 ml/ml/min and 0.2300 ± 0.1206 ml/ml/min, respectively. The physiological noise is about 3.4 times higher than thermal noise although this value is affected by the size of ROI for each breathhold. Note that the effect of thermal noise decreases systematically with larger ROI size; however, this is not the case for physiological noise, as it is expected to have spatial correlation.

Figure 2 contains an illustration of the septal ROI, and a plot of resting MBF measurements from one volunteer (top row of Table 1) as a function of the number of voxels averaged. For this particular subject, the total number of voxels over six breathholds was 483 and measured SNR was 73.9. With these parameters, the calculated probability of measured MBF error being <0.1 ml/ml/min was 96.1% based on thermal-noise only, but was 94.0% when accounting for physiologic noise.

Figure 3 shows six MBF measurements averaged for each breathhold in time order from the same subject. As specified earlier, the order of control and tagged image acquisitions alternated, with {tagged, control} in the odd

Table 1
MBF Measurements in Healthy Volunteers at Rest*

Age (years) and gender (M/F)	MBF (ml/ml/min)	SNR (B/σ_N)	ROI size (cm^3)	Thermal noise only		Physiological noise	
				$\sigma_{MBF,T}$ (ml/ml/min)	Confidence (%)	$\sigma_{MBF,P}$ (ml/ml/min)	Confidence (%)
29 M	0.74	73.9	3.50	0.048	96.1	0.053	94.0
31 F	0.83	55.9	1.35	0.096	70.5	0.090	73.6
28 F	1.11	80.5	2.10	0.060	90.6	0.219	35.3
33 M	1.16	42.5	2.55	0.094	71.2	0.181	42.0
28 F	1.16	75.8	3.47	0.046	97.0	0.113	62.6
34 M	1.17	66.6	2.35	0.071	84.3	0.146	50.6
31 M	1.21	50.0	2.45	0.097	70.0	0.331	23.7
34 M	1.27	63.4	6.53	0.041	98.5	0.201	38.1
31 M	1.33	68.3	2.42	0.064	88.4	0.160	46.8
33 M	1.37	43.3	3.73	0.086	75.8	0.279	28.0
32 M	1.60	80.6	4.08	0.053	94.0	0.432	18.2
35 M	1.62	68.0	3.00	0.056	92.8	0.239	32.4
35 M	1.77	50.5	3.12	0.073	82.9	0.180	42.2
29 M	1.85	55.8	2.92	0.077	80.5	0.434	18.2
31 M	2.25	81.6	2.83	0.061	89.6	0.392	20.2
Average	1.36	63.8	3.09	0.068	85.5	0.230	41.7

*Columns contain the measured MBF, SNR, size of the septal ROI, SD of measured MBF, and confidence (probability of measured MBF error being < 0.1 ml/ml/min) from 15 scans of healthy subjects. Data are sorted in ascending order according to MBF.

breathholds and {control, tagged} in the even breathholds. Note that the MBF measurements from {tagged, control} pairs are always higher than those from {control, tagged} pairs. This error appears to stem from incomplete static tissue cancellation due to time delay of 6 s, which is insufficient for the full relaxation of longitudinal magnetization. Based on Bloch simulation and Eq. [1], the MBF error caused by a 6-s time delay is ± 0.25 ml/ml/min for the heart rate of this subject, which appears consistent with the pattern of oscillation seen in Fig. 3. This effect is best seen in this particular dataset because it exhibited the lowest temporal noise of our 15 scans.

Dependence on Inflow

Table 2 contains MBF measurements from five subjects in which the thickness of the control image inversion slab was modified to include just the imaging slice, the entire left ventricle, and everything. In all subjects, thickening the inversion slab reduced measured MBF. The average change in MBF with inversion of the left ventricle and everything with respect to regular MBF were –68% and –92%, respectively. This matched our expectation that excluding blood in the coronaries from tagging would result in lower estimated MBF than that from including all out-of-slice blood, and supports the notion that the ASL signal measured by this approach is dominated by inflow.

Modulation With Mild Stress

Table 3 contains MBF measurements from seven subjects at rest and with two forms of mild stress, passive leg elevation and handgrip at 40% of MVC. The average heart rate change from rest was –1% with leg elevation and 0.3%

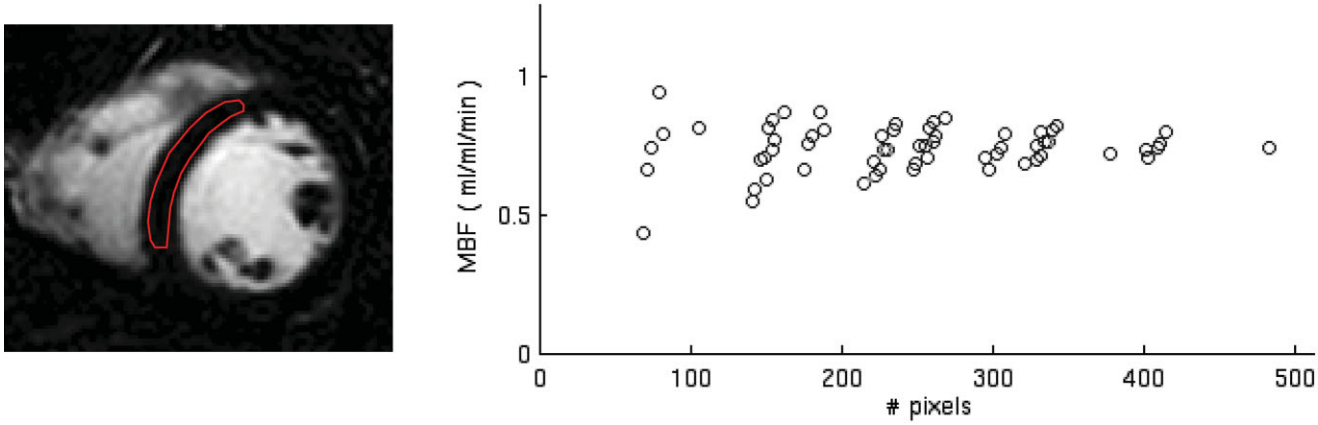

FIG. 2. MBF measurement from the ventricular septum of one subject. (Left) Illustration of the septal ROI that is manually segmented based on ASL difference images. The ROI volume was 3.50 cm^3. (Right) Measured resting MBF as a function of the number of voxels averaged. Roughly 50 voxels were segmented for each breathhold, resulting in a measurement of 0.74 ml/ml/min based on six breathholds (rightmost data point). All other data points were simulated by considering subsets of the six breathholds. [Color figure can be viewed in the online issue, which is available at www.interscience.wiley.com.]

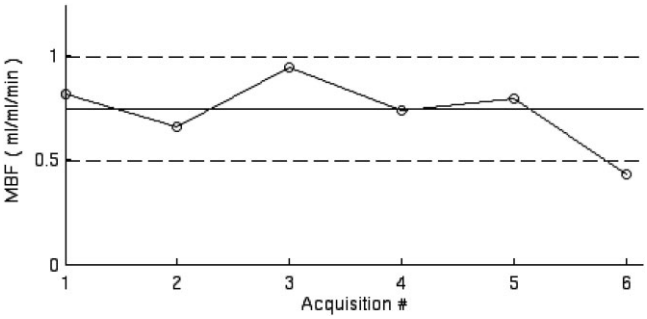

FIG. 3. Six MBF measurements averaged for each breathhold with alternating control/tagging image order. The solid line in the middle corresponds to the MBF value averaged over all voxels from six breathholds (0.74 ml/ml/min), and two dotted lines represent estimated upper (0.74 + 0.25 ml/ml/min) and lower (0.74 – 0.25 ml/ml/min) bounds of signal deviation due to incomplete static tissue relaxation.

with handgrip. MBF measurements during leg elevation and handgrip were higher than MBF measurement at rest in five subjects, comparable in one subject, and lower in one subject. The average increases in MBF were 30% and 29% with leg elevation and handgrip, respectively. These results are comparable to those in Refs. 25 and 26 where ABF during passive leg elevation increased by roughly 16%, and MBF during handgrip increased by roughly 35%. The 29% increase of MBF with handgrip is statistically significant ($P = 0.045$) while the 30% increase of MBF with leg elevation is not statistically significant ($P = 0.157$), largely due to the outlier result from the fourth volunteer.

DISCUSSION

This study demonstrates that subtractive myocardial ASL at 3T with pulsed tagging and SSFP imaging yields a distinct and measurable signal in human myocardium. In healthy volunteers, this signal is consistent with MBF ranges established using ^{13}N-ammonia PET, and shows a tendency to be inflow-dependent and modulate as expected with mild forms of stress. This study supports the feasibility of quantifying MBF in humans noninvasively using ASL.

This study has also determined that myocardial ASL MRI is limited by SNR. Although normal MBF is roughly twice as high as normal cerebral blood flow (CBF) (30,31), the intrinsic myocardial SNR when using modern eight-channel cardiac coils is roughly three times lower than gray matter SNR when using modern eight-channel head coils (measured on our 3T scanner in three healthy volunteers), primarily due to the larger noise-producing volume. This results in the need for a higher number of signal averages in myocardial ASL, compared to brain ASL, in order to achieve diagnostically useful confidence. Furthermore, because it is not practical to use 50+ repetitions in myocardial ASL (equal to the number of breathholds), spatial signal averaging is also required. The current spatial resolution of our MBF measurements is roughly 3 cm^3 (much larger than the resolution of the base images, $2.5 \times 2.5 \times 10$ mm^3) due to this need for spatial signal averaging.

As an alternative to voxelwise myocardial perfusion mapping, ROI-based analysis appears to be feasible, with segmental resolution similar to the standard 17-segment model (32). Figure 4 contains a voxelwise perfusion map from one breathhold, and a ROI-based perfusion map from 20 breathholds for comparison, both from the same healthy volunteer that exhibited moderate physiologic noise ($\sigma_{MBF,P} = 0.069$ ml/ml/min for the entire myocardium). For the ROI-based perfusion map, only endocardial and epicardial borders from each breathhold were delineated manually based on the difference image, and the circumference of the left ventricle was automatically divided into eight segments. Signal averaging was performed within each segment over multiple breathholds, yielding one MBF estimate that represents each segment. This way, even with the rather low SNR of myocardial ASL, the current approach may provide a perfusion map that is of diagnostic value, without requiring image registration for signal averaging.

Improvements in SNR efficiency will of course benefit ROI-based perfusion mapping, and will enable shorter scans, smaller ROIs, and tighter confidence intervals. Myocardial SNR is expected to be increased 50–75% with emerging 16- and 32-channel cardiac coils (33). Furthermore the SNR of myocardial ASL can be expected to improve with the development of more efficient tagging schemes (specific to the heart) and with the development of image acquisition methods optimized for detecting the ASL signal, both of which remain as future work.

Physiological noise (sometimes called temporal noise) is a crucial factor in myocardial ASL mostly due to breathing motion. Our preliminary estimates suggest that physiological noise in these studies was approximately 3.4 times

Table 2
MBF Measurements With Different Slab-Selective Inversion Thicknesses*

Age (years) and gender (M/F)	FAIR	Tag excludes LV		Null tag	
		MBF (ml/ml/min)	Change (%)	MBF (ml/ml/min)	Change (%)
31 M	1.21	0.36	−70	0.17	−86
28 F	1.16	0.64	−45	0.11	−91
29 M	1.85	0.83	−55	−0.36	−119
32 M	1.60	0.13	−92	0.69	−57
34 M	1.17	0.25	−79	−0.07	−106
Average	1.40	0.44	−68	0.11	−92

*FAIR = 3 cm, Tag excludes LV = 12 cm, Null tag = nonselective.

Table 3
MBF Measurements at Rest, With Passive Leg Elevation and With Isometric Handgrip Exercise, and Heart Rates for Each Study*

Age (years) and gender (M/F)	Resting MBF (HR)	Leg elevation		Handgrip	
		MBF (HR)	MBF change (%)	MBF (HR)	MBF change (%)
29 M	0.74 (62)	0.99 (60)	34	0.98 (62)	32
31 F	0.83 (50)	1.31 (52)	58	1.25 (52)	51
28 F	1.11 (68)	1.83 (71)	65	1.57 (75)	41
31 M	1.33 (64)	0.96 (68)	−28	1.17 (64)	−12
32 M	1.03 (68)	1.06 (64)	3	1.31 (67)	27
29 M	1.04 (66)	1.08 (56)	4	1.01 (60)	−3
32 M	0.50 (69)	0.87 (71)	74	0.84 (68)	68
Average	0.94 (64)	1.16 (63)	30	1.16 (64)	29

*Average heart rate change from rest was −1% with leg elevation and 0.3% with handgrip. MBF measurements are in ml/ml/min and HR is in beats per minute (bpm).
HR = heart rate.

higher than the level of thermal noise, which would suggest the use of far more than six breathholds. However, the SD of the physiological noise distribution over different subjects was also 6.5 times higher than that of thermal noise only. This indicates that the number of breathholds needed for confidence in the derived MBF measurement will vary significantly across subject, while thermal noise is relatively consistent over different subjects and can yield <0.1 ml/ml/min error with 85.5% confidence with six breathholds. This provides strong motivation for future investigation of background suppression (BGS) schemes and novel tagging schemes that have the potential to reduce physiological noise.

One important drawback of FAIR tagging (or any slab-selective tag of the proximal aorta in the short-axis plane) is that the tagged region includes blood in the left atrium and possibly a portion of the left ventricle. This results in spurious ASL signal in the LV blood pool that may interfere with measurement of the myocardial ASL signal. The effect is most readily apparent in difference images, where the LV blood pool is typically 30–40 times brighter than adjacent myocardium. One possible solution is to apply diffusion sensitizing gradients (DSG) with low diffusion weighting to dephase blood flow (34) immediately prior to image acquisition in both control and tagged images. While this is a simple solution to suppress signal from the LV blood pool, it has a disadvantage that the tagged blood in the myocardium experiences signal attenuation due to T_2 relaxation and motion-related dephasing, leading to SNR loss. LV blood in the ASL difference image can also be suppressed by more sophisticated tagging scheme such as one that selectively excludes the left atrium and left ventricle while tagging the proximal aorta. Suppression of the LV blood signal is likely to reduce physiological noise and allow the use of larger myocardial ROIs while avoiding partial volume effects in voxels along the endocardial border.

Unlike brain ASL, image acquisition in the steady state is difficult for myocardial ASL because the duration of breathholds is limited and the heart rate can vary during a scan session. We chose a multiple breathhold strategy, where each breathhold contained a pair of control and tagged images with time delay of 6 s between them. In order to compensate for MBF measurement error caused by incomplete relaxation, we alternated the order of control and tagged images, and used an even number of breathholds. It is possible to use longer time delays between tagged and control images (e.g., 10 s) to provide more complete relaxation; however, this increases the duration of each breathhold, which increases the possibility of misregistration and changes in the T_1 of blood due to deoxygenation. In our experience, alternating the order of the tagged and control images proved to be a simple and effective way to mitigate error caused by incomplete relaxation. Ultimately, free-breathing methods employing ad-

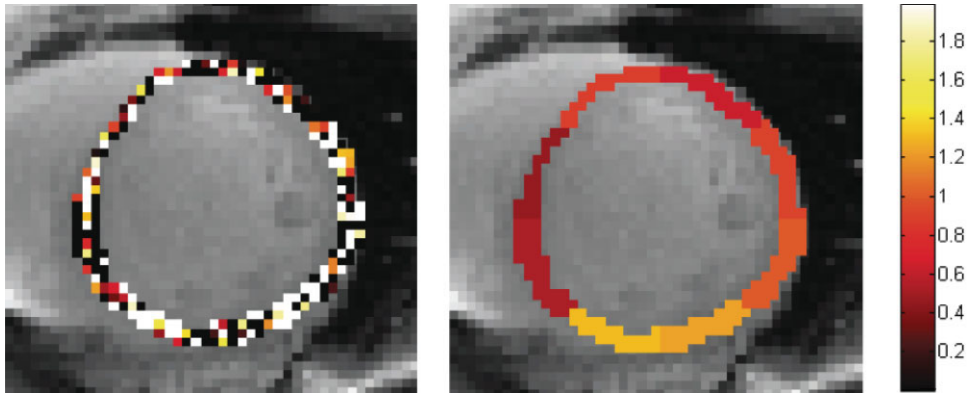

FIG. 4. MBF maps (ml/ml/min) from one healthy volunteer with moderate physiological noise. (Left) Voxelwise MBF map from one breathhold (values < 0.0 appear black, values > 2.0 appear white). (Right) ROI-based MBF map from 20 breathholds (LV myocardium is divided into eight radial segments).

vanced prospective gating and tracking may be necessary for routine application of myocardial ASL in patients.

Brain ASL has evolved over the past 15 to 20 years, and many important innovations can be applied to myocardial ASL. For instance, BGS has proved useful for the reduction of physiological noise in brain ASL (35–38), and may also be beneficial in myocardial ASL where breathing motion is significant. Also, pseudocontinuous tagging (39), which provides the highest tagging efficiency among existing brain ASL methods, may be applied to myocardial ASL, as a means to improve SNR. In this case, the spatial placement and the timing of flow-driven tagging pulses should be optimized to the coronary artery geometry and pulsatile flow pattern, in order to produce the highest tagging efficiency.

The validation of myocardial ASL in humans is complicated by cardiac and respiratory motions, and the lack of an established ground truth with which to compare the results from proposed method. This is quite different from animal studies, where sedation is possible and results can be compared with invasive microsphere-based blood flow measurement. A definitive validation of proposed methods against a gold standard such as ^{13}N-ammonia PET would be a natural follow-up to this study.

CONCLUSIONS

We have demonstrated the feasibility of myocardial blood flow assessment in humans, using ASL at 3T. MBF measurements in healthy volunteers at rest were consistent with MBF ranges established by the quantitative PET literature. These MBF measurements were inflow-dependent, and increased by 30% and 29% with passive leg elevation and handgrip stress, respectively, as expected. This study also demonstrates that myocardial ASL is limited by SNR, and that accurate perfusion assessment with the technique is currently limited to ROI analysis. Sources of physiological (nonthermal) noise and suppression techniques remain to be explored. There is substantial opportunity for improved tagging and imaging methods that may strengthen the myocardial ASL signal while reducing temporal noise.

REFERENCES

1. Schwitter J, Nanz D, Kneifel S, Bertschinger K, Buchi M, Knusel PR, Marincek B, Luscher TF, von Schulthess GK. Assessment of myocardial perfusion in coronary artery disease by magnetic resonance: a comparison with positron emission tomography and coronary angiography. Circulation 2001;103:2230–2235.
2. Nagel E, Klein C, Paetsch I, Hettwer S, Schnackenburg B, Wegscheider K, Fleck E. Magnetic resonance perfusion measurements for the noninvasive detection of coronary artery disease. Circulation 2003;108:432–437.
3. Wagner A, Mahrholdt H, Holly TA, Elliott MD, Regenfus M, Parker M, Klocke FJ, Bonow RO, Kim RJ, Judd RM. Contrast enhanced MRI and routine single photon emission computed tomography (SPECT) perfusion imaging for detection of subendocardial myocardial infarcts: an imaging study. Lancet 2003;361:374–379.
4. Jerosch-Herold M, Seethamraju RT, Swingen CM, Wilke NM, Stillman AE. Analysis of myocardial perfusion MRI. J Magn Reson Imaging 2004;19:758–770.
5. DiBella EV, Parker DL, Sinusas AJ. On the dark rim artifact in dynamic contrast enhanced MRI myocardial perfusion studies. Magn Reson Med 2005;54:1295–1299.
6. Mühling OM, Dickson ME, Zenovich A, Huang Y, Wilson BV, Wilson RF, Anand IS, Seethamraju RT, Jerosch-Herold M, Wilke NM. Quantitative magnetic resonance first-pass perfusion analysis: inter- and intraobserver agreement. J Cardiovasc Magn Reson 2001;3:247–256.
7. Sieber MA, Lengsfeld P, Walter J, Schirmer H, Frenzel T, Siegmund F, Weinmann HJ, Pietsch H. Gadolinium-based contrast agents and their potential role in the pathogenesis of nephrogenic systemic fibrosis: the role of excess ligand. J Magn Reson Imaging 2008;27:955–962.
8. Noeske R, Seifert F, Rhein KH, Rinneberg H. Human cardiac imaging at 3T using phased-array coils. Magn Reson Med 2000;44:978–982.
9. Williams DS, Grandis DJ, Zhang W, Koretsky AP. Magnetic resonance imaging of perfusion in the isolated rat heart using spin inversion of arterial water. Magn Reson Med 1993;30:361–365.
10. Kober F, Iltis I, Cozzone PJ, Bernard M. Myocardial blood flow mapping in mice using high-resolution spin labeling magnetic resonance imaging: influence of ketamine/xylazine and isoflurane anesthesia. Magn Reson Med 2005;53:601–606.
11. Bauer WR, Roder F, Hiller KH, Han H, Fröhlich S, Rommel E, Haase A, Ertl G. The effect of perfusion on T_1 after slice-selective spin inversion in the isolated cardioplegic rat heart: measurement of a lower bound of intracapillary-extravascular water proton exchange rate. Magn Reson Med. 1997;38:917–923.
12. Wacker CM, Fidler F, Dueren C, Hirn S, Jakob PM, Ertl G, Haase A, Bauer WR. Quantitative assessment of myocardial perfusion with a spin-labeling technique: preliminary results in patients with coronary artery disease. J Magn Reson Imaging 2003;18:555–560.
13. Zhang H, Shea SM, Park V, Li D, Woodard PK, Gropler RJ, Zheng J. Accurate myocardial T_1 measurements: toward quantification of myocardial blood flow with arterial spin labeling. Magn Reson Med 2005;53:1135–1142.
14. Zhang H, Gropler R, Woodard P, Zheng J. Myocardial perfusion measurement with arterial spin labeling at 3T: a comparison with 1.5T. In: Proceedings of the 15th Annual Meeting of ISMRM, Berlin, Germany, 2007 (Abstract 3613).
15. Poncelet BP, Koelling TM, Schmidt CJ, Kwong KK, Reese TG, Ledden P, Kantor HL, Brady TJ, Weisskoff RM. Measurement of human myocardial perfusion by double-gated flow alternating inversion recovery EPI. Magn Reson Med 1999;41:510–519.
16. An J, Voorhees A, Chen Q. SSFP arterial spin labeling myocardial perfusion imaging at 3 Tesla. In: Proceedings of the 13th Annual Meeting of ISMRM, Miami Beach, FL, USA, 2005 (Abstract 253).
17. Kwong KK, Chesler DA, Weisskoff RM, Donahue KM, Davis TL, Ostergaard L, Campbell TA, Rosen BR. MR perfusion studies with T_1-weighted echo planar imaging. Magn Reson Med 1995;34:878–887.
18. Kim S-G. Quantification of regional cerebral blood flow change by flow-sensitive alternating inversion recovery (FAIR) technique: application to functional mapping. Magn Reson Med 1995;34:293–301.
19. Martirosian P, Klose U, Mader I, Schick F. FAIR True-FISP perfusion imaging of the kidneys. Magn Reson Med 2004;51:353–361.
20. Nishimura DG, Vasanawala SS. Analysis and reduction of the transient response in SSFP imaging. In: Proceedings of the 8th Annual Meeting of ISMRM, Denver, CO, USA, 2000 (Abstract 301).
21. LeRoux P. Simplified model and stabilization of SSFP sequences. J Magn Reson 2003;163:23–37.
22. Pruessmann KP, Weiger M, Scheidegger MB, Boesiger P. SENSE: Sensitivity encoding for fast MRI. Magn Reson Med 1999;42:952–962.
23. Roemer PB, Edelstein WA, Hayes CE, Souza SP, Mueller OM. The NMR phased array. Magn Reson Med 1990;16:192–225.
24. Graves MJ, Emmens D, Lejay H, Hariharan H, Polzin J, Lomas DJ. T_2 and T_2* quantification using optimal B_1 image reconstruction for multicoil arrays. J Magn Reson Imaging 2008;28:278–281.
25. Buxton RB, Frank LR, Wong EC, Siewert B, Warach S, Edelman RR. A general kinetic model for quantitative perfusion imaging with arterial spin labeling. Magn Reson Med 1998;40:383–396.
26. Kivowitz C, Parmley WW, Donoso R, Marcus H, Ganz W, Swan HJ. Effects of isometric exercise on cardiac performance. The grip test. Circulation 1971;44:994–1002.
27. Helfant RH, De Villa MA, Meister SG. Effect of sustained isometric handgrip exercise on left ventricular performance. Circulation 1971;44:982–993.

28. Lowe DK, Rothbaum DA, McHenry PL, Corya BC, Knoebel SB. Myocardial blood flow response to isometric (handgrip) and treadmill exercise in coronary artery disease. Circulation 1975;51:126–131.
29. Lafanechère A, Pène F, Goulenok C, Delahaye A, Mallet V, Choukroun G, Chiche JD, Mira JP, Cariou A. Changes in aortic blood flow induced by passive leg raising predict fluid responsiveness in critically ill patients. Crit Care 2006;10:R132.
30. Chareonthaitawee P, Kaufmann PA, Rimoldi O, Camici PG. Heterogeneity of resting and hyperemic myocardial blood flow in healthy humans. Cardiovasc Res 2001;50:151–161.
31. Ibaraki M, Miura S, Shimosegawa E, Sugawara S, Mizuta T, Ishikawa A, Amano M. Quantification of cerebral blood flow and oxygen metabolism with 3-dimensional PET and 15O: validation by comparison with 2-dimensional PET. J Nucl Med 2008;49:50–59.
32. Cerqueira MD, Weissman NJ, Dilsizian V, Jacobs AK, Kaul S, Laskey WK, Pennell DJ, Rumberger JA, Ryan T, Verani MS. Standardized myocardial segmentation and nomenclature for tomographic imaging of the heart: a statement for healthcare professionals from the Cardiac Imaging Committee of the Council On Clinical Cardiology of the American Heart Association. Circulation 2002;105:539–542.
33. Hardy CJ, Cline HE, Giaquinto RO, Niendorf T, Grant AK, Sodickson DK. 32-element receiver-coil array for cardiac imaging. Magn Reson Med 2006;55:1142–1149.
34. Okada Y, Ohtomo K, Kiryu S, Sasaki Y. Breath-hold T_2-weighted MRI of hepatic tumors: value of echo planar imaging with diffusion-sensitizing gradient. J Comput Assist Tomogr 1998;22:364–371.
35. Ye FQ, Frank JA, Weinberger DR, McLaughlin AC. Noise reduction in 3D perfusion imaging by attenuating the static signal in arterial spin tagging (ASSIST). Magn Reson Med 2000;44:92–100.
36. Duyn JH, Tan CX, van Gelderen P, Yongbi MN. High-sensitivity single-shot perfusion-weighted fMRI. Magn Reson Med 2001;46:88–94.
37. Garcia DM, Duhamel G, Alsop DC. Efficiency of inversion pulses for background suppressed arterial spin labeling. Magn Reson Med 2005; 54:366–372.
38. Wong EC, Cronin M, Wu W-C, Inglis B, Frank LR, Liu TT. Velocity selective arterial spin labeling. Magn Reson Med 2006;55:1334–1341.
39. Garcia DM, de Bazelaire C, Alsop D. Pseudo-continuous flow driven adiabatic inversion for arterial spin labeling. In: Proceedings of the 13th Annual Meeting of ISMRM, Miami Beach, FL, USA, 2005 (Abstract 37).